Int J Clin Exp Pathol 2022;15(3):97-109
www.ijcep.com /ISSN:1936-2625/IJCEP0121113

Original Article

Secondary injury and pro-inflammatory macrophages increase osteophyte growth and fracture healing in canine atrophic nonunion

Jingxin Pan[1], Ying Gao[2], Zhijun Pan[3], Kaikai Lu[4], Junjun Fan[1], Chunmei Wang[1], Zhilong Hao[1], Zewei Li[1], Taoran Wang[1], Zhi Yuan[1]

[1]The Air Force Military Medical University, Xi'an 710032, Shaanxi, China; [2]Medical College of Yan'an University, Shaanxi, China; [3]4th Hospital of Yulin, Yulin 719000, Shaanxi, China; [4]Department of medicine, Xi'an Jiaotong University, Xi'an, Shaanxi, China

Received August 26, 2020; Accepted January 18, 2022; Epub March 15, 2022; Published March 30, 2022

Abstract: Objectives: In this study, we used a canine high-energy fracture model to examine the relationship between the early inflammatory reaction in adjacent tissues and the ability for osteophyte growth, aiming to identify causes that lead to atrophic nonunion inflammatory disease and to provide new strategies for prevention and treatment. Materials and methods: Forty-eight models of canine femoral high energy fractures were prepared and randomly divided into groups A and B (n=24 in each group). Dogs in both groups underwent open reduction and 6-hole plate internal fixation. Group A models were re-opened, and muscle near the bone was scraped at 14 d after the operation. On days 3, 17, 28, and 42 after fracture, 6 experimental dogs were euthanized per group, and the fracture specimens were used to examine pathologic changes and the growth of callus in the fractured end and its adjacent tissues. Results: At day 14, neutrophil infiltration, with no macrophage recruitment, no mesenchymal cell proliferation, and no fracture healing cascade were observed in the adjacent tissues of both groups. Immediately after the second injury was performed in group A, many macrophages were seen, and mesenchymal cells proliferated, which initiated vigorous osteophyte growth and led to osteophyte healing. Atrophic nonunion was observed in group B without secondary injury. Conclusion: Macrophage recruitment deficiency in adjacent soft tissue in early surgery for high-energy fractures may be an important cause of atrophic nonunion. Secondary injury inflammation can effectively recruit mononuclear macrophages, generate osteoclasts, re-initiate the growth of osteophytes, and promote fracture healing.

Keywords: Canine femoral high energy fracture model, atrophic nonunion, secondary injury, macrophage, new callus

Introduction

With the rapid development of modern industry and transportation, high energy fractures continue to increase. The incidence of multiple injuries and fractures has also been increasing, especially in critically injured patients. High-energy fractures, multiple fractures, and multiple injuries with fractures are prone to boneless growth, which ultimately leads to atrophic nonunion [1-4]. The exact mechanism and causes leading to atrophic nonunion are not fully understood.

Previous studies suggested that inadequate blood supply to the fracture and mechanical instability may be the main cause of atrophic nonunion [2, 4]. Reed *et al*. reported no ischemia at the fracture sites with atrophic nonunion [5], suggesting that blood supply deficiency may not be the only cause. Moreover, mechanical stability may not be indefinitely achieved in clinical practice. Also, Bastian *et al.* pointed out that the early inflammatory phase of fracture healing initiates the healing process and guides a series of processes [6]. Fracture healing may be impaired if the process is interrupted by a systemic inflammatory reaction or excessive local inflammatory reaction [6]. Loi et al. pointed out that if the inflammatory response caused by fracture is well-controlled during the acute phase, it can promote healing; if the

acute phase is inhibited, chronic inflammation may appear, affecting the healing process [7]. Bleek *et al.* proposed that the initiation process of fracture healing is an immune process. Early hematoma formation after the fracture indicates the beginning of the inflammatory reaction. Pre-inflammatory stimulation activates the coagulation cascade and activates neutrophils, monocytes, and macrophages, and simultaneously, the fracture healing cascade [8, 9].

Most high-energy fractures are open comminuted fractures, whose damage is mostly concealed by exterior phenomena such as open pollution and fracture comminution. As muscle contusion is not easily monitored, its damage to the fracture healing tends to remain neglected. It is believed that during high-energy fractures, too much impact energy is released during the original impact, causing extensive tissue damage; however, the true degree of damage is not proportional to the degree of open comminution and may appear as a simple closed fracture. It has been suggested that high-energy fractures are associated with both blood supply damage and a strong inflammatory reaction, which affects the micro-environment of the fracture repair, thus impairing the ability for fracture healing [6-11].

In our previous study, we established an experimental model of canine femoral high energy fracture [10], leading to local severe inflammation. Adjacent muscles were severely stabbed with bone ends to simulate extensive soft tissue damage (intraosseous blood supply and bone marrow were not damaged) of high-energy fractures to study the local inflammation. Open reduction and 6-hole plate internal fixation produced marked local inflammation, which resulted in atrophic nonunion. However, for the same degree of original damage and surgical injury, if the surgery was delayed for 7 days, only mild local inflammation was observed and fracture healing was observed [10]. These results suggest that mild inflammation in the early stage of fracture promotes healing, but early severe inflammation prevents fracture healing.

Establishing an atrophic nonunion and dystrophic nonunion animal model may be very challenging due to small rodents' strong callus growth ability; therefore, large animals are often chosen for research purposes. In our preliminary experiment, we examined high-energy fractures in sheep. Our data suggested that the femoral bone cortex of sheep was thin and brittle, and fixing plate screws was challenging. Moreover, a vigorous callus growth was observed, and it was challenging to induce nonunion. However, the cortex of the canine femur bone was found to be thick and hard. We were able to firmly fix the plate and screws to the bone. The bone growth was slow, which is similar to humans.

In this study, we used this model to examine further the relationship between the early inflammatory reaction of adjacent tissues and the ability for osteophyte growth, aiming to identify new causes that lead to atrophic nonunion inflammatory disease and to provide new strategies for prevention and treatment of atrophic nonunion.

Materials and methods

Experimental animals

Forty-eight normal adult female beagle dogs (age 4-6 years old, weight 8-12 kg with an average of 9.0 ± 1.5 kg) were selected for this study. Femur length was 110-150 mm (distance between the large trochanter and the external femoral condyle) with a diameter of 12-15 mm (measured with a scale to measure the diameter of the fracture end during surgery). All animals were housed in an environment with a temperature of 23 ± 3°C, relative humidity of 40-70%, and a light/dark cycle of 12/12 hr and fed with 500 g of experimental dog food per day in the morning; all animals had free access to water.

Animal grouping was randomized, with no difference in age and weight between groups. Animals had no trauma, infection, or malformation and no other systemic diseases. In addition, all animals were kept by the same breeder.

The experimental animals were provided by the Experimental Animal Center of Xi'an Jiaotong University. This study was approved by the ethics committee of Xi'an Jiaotong University (No. 2019-959). All experimental procedures were in accordance with the Animal Experiment Guidelines of Xi'an Jiaotong University and were

in line with international animal ethics standards.

Steel plate

A self-made plate with 6 holes customized with 00Cr18Ni14Mo3 stainless steel material (length: 60 mm (2/5 of the average length of the femur); width: 8 mm (1/4 of the bone circumference); thickness: 3 mm) conforming to GB 4234 standards was adopted. The plates were manufactured by Suzhou Xinrong Bolt Medical Devices Co. Ltd. (Zhangjiagang city, Jiangsu Province).

Study design

This experiment was set as a randomized controlled animal experiment. Forty-eight experimental models were prepared as previously described [10]. Briefly, a simple fracture of the closed femur of the dog was artificially made by puncturing the periosteum and muscle around the bone end 10 times. The puncture depth was 4 cm overlapping the bone end, and the total depth on both sides was 8 cm. Animals were then randomized into group A and B (n=24 in each group). Animals in both groups were treated with open reduction and received a 6-hole plate internal fixation.

Animals in group A received re-resection 14 days after the operation (which was not performed for group B). Briefly, after anesthesia, the original incision was cut again; the muscle was cut straight to the fracture. As the hematoma was absorbed, excessive inflammation was observed in the periosteum and muscles that temporarily lost the chemotactic ability of stem cells (comparable to group B). In addition, no organic tissue was generated, so the adjacent muscle was not connected to the bone end. The periosteum detacheres (15 mm in width) were then inserted between the muscle and the bone, and the muscle was scraped three times toward the surface of the bone. The scraping range was 3 cm, i.e., 1.5 cm above and below the fracture line (meanwhile, a small amount of muscle tissue was taken for examination), and then the incision layer was sutured by layer. The periosteum and muscle that were subjected to excessive inflammation and recovered from the inflammation remained in a state of quiescence or non-healing. Moreover, the inflammation secondary to injury mostly came from soft tissue incision injury instead of the periosteum and muscle.

The same surgical team performed experimental operations for both groups. All animals that underwent open reduction or secondary incision were treated with a local injection of 4 mg of renin-salt saline to stop bleeding. No antibiotics or anti-inflammatory drugs were used after surgery. The animals were free to move, the limbs were not broken, and at early stages, limbs were mostly suspended, and animals were carefully fed.

The animals were sacrificed intravenously with 500 mg thiopental (Shanghai Xinya Pharmaceutical Co. Ltd.). Then, 20 ml of 10% potassium chloride was injected intravenously to stop the heartbeat.

Gross specimen observation

General conditions of the animals, including diet, activity, local wound healing, and swelling of the affected limb, were observed and recorded. After tissues were taken, formation of the callus was observed.

Biomechanical testing

Two groups of 6-week-old animals were chosen to measure the overall femoral specimens. Youhong 504e three-point bending tester (Shanghai Youhong Testing Technology Co., Ltd.) was adopted to conduct a three-point bending stress test at the fracture site, and the maximum limit bending stress value was recorded. Mean values were compared.

X-ray examination

Before performing euthanasia, the affected limbs were examined in two groups at weeks 2 and 6 following fracture by digital X-ray imaging to observe the callus status. A square grid with a side length of 1 mm was used to measure the number of grids with bone defection for statistical analyses.

Radiology scanning analysis

The metabolic activity of the bones at the fractured end in two groups was analyzed using ^{99m}Tc flash scan at 3 d, 7 d, 14 d, 21 d, and 28 d after a fracture. Four dogs were chosen from each group. At 3 d, inflammatory bone metabo-

lism did not increase. Osteuclide reflected the blood supply changes at the bone end. At 7 d, the inflammatory bone metabolism increased from the sides away from the bone end, while at 14 d, 21 d, and 28 d, bone metabolism advanced to the bone end.

Light microscopy analysis of tissue section

At 3 d, 17 d, 28 d, and 42 d after the fracture, 6 animals from each group were chosen. The fracture specimens were taken (the adjacent muscles were taken during bone dissection at two weeks in group A), and the growth of the fracture end and its adjacent tissues was observed. The specimens were fixed in 10% formalin at room temperature for over 24 hours, and then H&E staining of paraffin sections (room temperature for 40 min; thickness 5 μm) and plastic section VG staining (room temperature for 30 min; thickness 30-50 μm) were performed to observe early inflammatory cell chemotaxis and growth of the callus. H&E staining was performed 3 days after surgery and 3 days after the second injury. The number of neutrophils and macrophages was counted from three different high-power fields of vision. The average value was recorded for statistical analysis.

Transmission electron microscopy observation

At 3 d and 17 d after the fracture, soft tissue specimens and bone specimens at 2 mm from the fracture end were obtained from two groups for cell growth observation. The tissue sample was immediately fixed in 2.5% glutaraldehyde fixative at 4°C for over 2 hours, dehydrated by ethanol gradient, followed by impregnation and embedding using epoxy resin Epon812. After polymerization, tissues were prepared for semi-ultra-thin sections with a thickness of 1-2 μm, and then methylene blue staining was performed, followed by light microscope location and slicing for 50-70 nm using Swedish LKB-V ultra-thin slicer. After staining by uranium acetate and lead citrate, a transmission electron microscope (Hitachi H-7650) was used for observation and photography. Photographs of the soft tissues were obtained by the electron microscope at a magnification of 4000X on day 3 after fracture and 3 days after secondary injury. The number of mesenchymal cells in 100 visual fields was counted for statistical analysis.

Statistical analysis

Continuous data conforming to a normal distribution are described as mean ± standard deviation (mean ± SD). SPSS 22.0 software (IBM Corp., Armonk, NY, USA) was used for statistical analyses. Student's *t*-test was used to explore differences between groups. *P*-values <0.05 were considered significant.

Results

The normal dietary habits and weight of animals increased by 0.5-1.7 kg two weeks before the sacrifice. Growth of the callus is shown in **Table 1**; histologic changes are presented in **Table 2**; radiologic results are shown in **Table 3**; electron microscope scan results are shown in **Table 4**. **Figures 1A**, **2A-D** and **3A-F** represent dog images in Group A, while **Figures 1B**, **1C**, **2E**, **2F** and **3G** are dog images in Group B.

Changes observed during first 14 days after fracture

The injury procedures and tissue responses were the same in the two groups. At 3 d after the fracture, the tissue produces much inflammation and neutrophils (extracellular nets) [12, 13]. In our previous study [10], we found no statistical difference in the number of neutrophils or macrophages between the two groups (P<0.01), and electron microscopy showed breaking scattered collagen fibers between muscle cells. In this study, no collagen fibers and mesenchymal cells were formed 14 d after fracture, and there was no osteophyte growth between the bone ends (**Figure 1B**). Apoptosis was not observed in osteocytes, and osteophyte growth was not initiated.

The radiologic scan showed no cold zone at the end of the fracture at 3 d (at this time, inflammatory bone metabolism was not increased), which appeared at 7 d (the bone metabolism began to increase; **Figure 4C**); at 14 d, the cold zone nearly disappeared (metabolism recovered, fracture gap was less than 5 mm, and radiologic scans were not displayed; **Figure 4F**; **Table 3**).

Changes observed 17 days after fracture

In group A (3 d after secondary injury), few neutrophils and a large number of macrophages

Table 1. Gross specimen observations at different days after fracture

Day after fracture/Group	3 d	17 d (3 d after second operation)	28 d (14 d after second operation)	42 d (28 d after second operation)
Group A	Abundantedema fluid	No edema fluid	Granulation covers bone end; epiphyses in fracture gap	Callus bridge
Group B	Abundant edema fluid	No liquid leakage, no granulation	Scar in the fracture gap	Atrophic absorption of the bone end; fracture space widened

Table 2. Histologic changes at different days

Day after fracture/Group	3 d	17 d (3 d after second operation)	28 d (14 d after second operation)	42 d (28 d after second operation)
Group A	A large number of neutrophils; No macrophages; No destruction of bone trabecular meshwork and blood supply	A small number of neutrophils; A large number of macrophages	Fracture space and external callus; coupling of bone formation to resorption	Callus bridging fracture space; coupling of bone formation to resorption; tunnel-like reconstruction
Group B	A large number of neutrophils; No macrophages; No destruction of bone trabecular meshwork and blood supply	Rich capillaries in adjacent tissues; No macrophages	Fracture space and external tissue organization; No callus; Scar	Scar barrier; sclerotic bone end internal bone reconstruction; no growth outside the bone end

Table 3. Radiologic scan results at different days in groups

Day after fracture/group	3 d	7 d	14 d	21 d	28 d
Group A	No metabolism increase at the end of the fracture; No cold zone	bone metabolism increase; relatively cold zone	Second operation Metabolism pushed on to the bone end; cold zone decrease	7 Metabolism increase; relatively cold zone	14 Cold zone disappears; Metabolism widened
Group B	No metabolism increase at the end of the fracture; No cold zone	bone metabolism increase; relatively cold zone	Metabolism pushed on to the bone end; cold zone decrease	fracture gap <1 cm; cold zone disappears	cold zone disappears; Metabolism not widened

Table 4. Electron microscope scan results at different days in groups

Day after fracture/group	3 d	17 d (3 d after second operation)	28 d (14 d after second operation)
Group A After secondary injury	A large amount of necrotic inflammatory cells; breaking scattered collagen fibers; Osteonecrosis	A large number of mesenchymal cells proliferate; collagen hyperplasia	A large amount of collagen outside the bone, Fibroblasts in the outer callus, Collagen fiber, Capillaries No osteoblasts in bone, osteocyte apoptosis
Group B	A large amount of necrotic inflammatory cells; breaking scattered collagen fibers; Osteonecrosis	No collagen outside the bone, no fibroblasts, no osteoblasts; osteoblasts in the bone, osteogenesis	No collagen outside the bone, no fibroblasts, no osteoblasts osteoblasts in the bone, osteogenesis

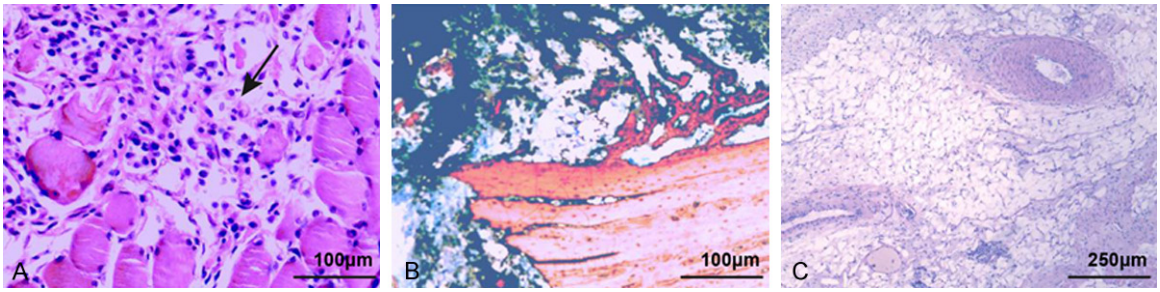

Figure 1. Tissue sections 17 d after the fracture. A. Secondary injury group (3 days after the second operation). A small number of neutrophils and a large number of macrophages in the adjacent tissue. H&E staining (40×). B. In the early surgery group, the fractured end was covered with tissue organization, with no osteoclasts, no coupling of bone formation to resorption, and no bone growth outside the fracture space and bone ends; VG staining (40×). C. Adjacent tissue without collagen fibrosis, tissue organization growth, rich capillaries, and boneless growth behavior; H&E staining (100×).

(**Figure 1A**) were observed, and electron microscopy results showed that mesenchymal cells began to proliferate. In group B, angiogenesis was observed, without inflammatory cell infiltration and mesenchymal cell proliferation (**Figure 1B**, **1C**). By light microscope macrophages and by electron microscope mesenchymal cells showed significant differences between the two groups (112 macrophages in group A, vs. 9 in group B, P<0.01).

Changes observed 28 days after fracture

In group A (14 d after the second injury), a tissue organization in the myocyte space was observed (**Figure 2D**). The tissue organization covered the bone end. The growth of callus and convergence was seen in the fracture space and around the bone end. A large number of macrophage fibroblasts was seen in the interstitial space in new bony trabeculae. Moreover, osteoclasts were seen on the trabecular bone wall (3 in group A vs. 0 in group B, P<0.01), and a large number of osteoblasts were also present (54 in group A vs. 7 in group B, P<0.01), similar to the coupling of bone formation to resorption (**Figures 2B**, **3A-C**).

Electron microscopy showed that adjacent tissue collagen fibers and mesenchyme continued to proliferate. Many osteoblasts, macrophages, and mesenchymal cells were observed in the callus of group A. In group B, a weak external callus appeared far from the fracture end; few osteoclasts and osteoblasts were observed, and the coupling of bone formation to resorption was extremely weak, and scars grew in the fracture space (**Figure 2E**, **2F**; **Tables 2**, **4**).

Changes observed 42 days after fracture

Callus healing in all 6 cases in group A transformed the nonunion model into a callus healing model. X-ray showed that callus (a number of couplings of bone formation to resorption) surrounded the fractured ends and completely filled the fracture gap, exceeding the average of the original bone ends by 11 grids. The maximum average bending stress was 172 N. In group B, atrophic nonunion was observed in all 6 cases, and the average bending stress value was zero, which was different from group A (172 in group A vs. 0 in group B, P<0.01). Scarring prevented the atrophy of the bone, and, in turn, atrophic nonunion emerged. The weak coupling of bone formation to resorption in the bone end only remodels the bone end itself and does not grow into the fracture space, resulting in sclerosis of the bone end; thus, the fracture gap widens. The area of bone absorption covered 39 grids; the average number of callus was 50 grids less than that in group A, with a difference (11 grids in group A vs. 39 grids in group B, with a difference of 50, P<0.01).

In this study, we presented the formation process and structure of the new callus. After the second injury, light and electron microscopy showed that the collagen fibers and fibroblasts (derived from mesenchymal cells) that make up the epiphyseal precursor tissue first formed at the edge of the soft tissue, which co-existed with muscle fibers (**Figure 2D**). Fibroblasts were transformed into chondrocytes after induction of osteogenic induction factor BMP, which was demonstrated to be derived from macrophages present at the fracture end (**Figure 3**)

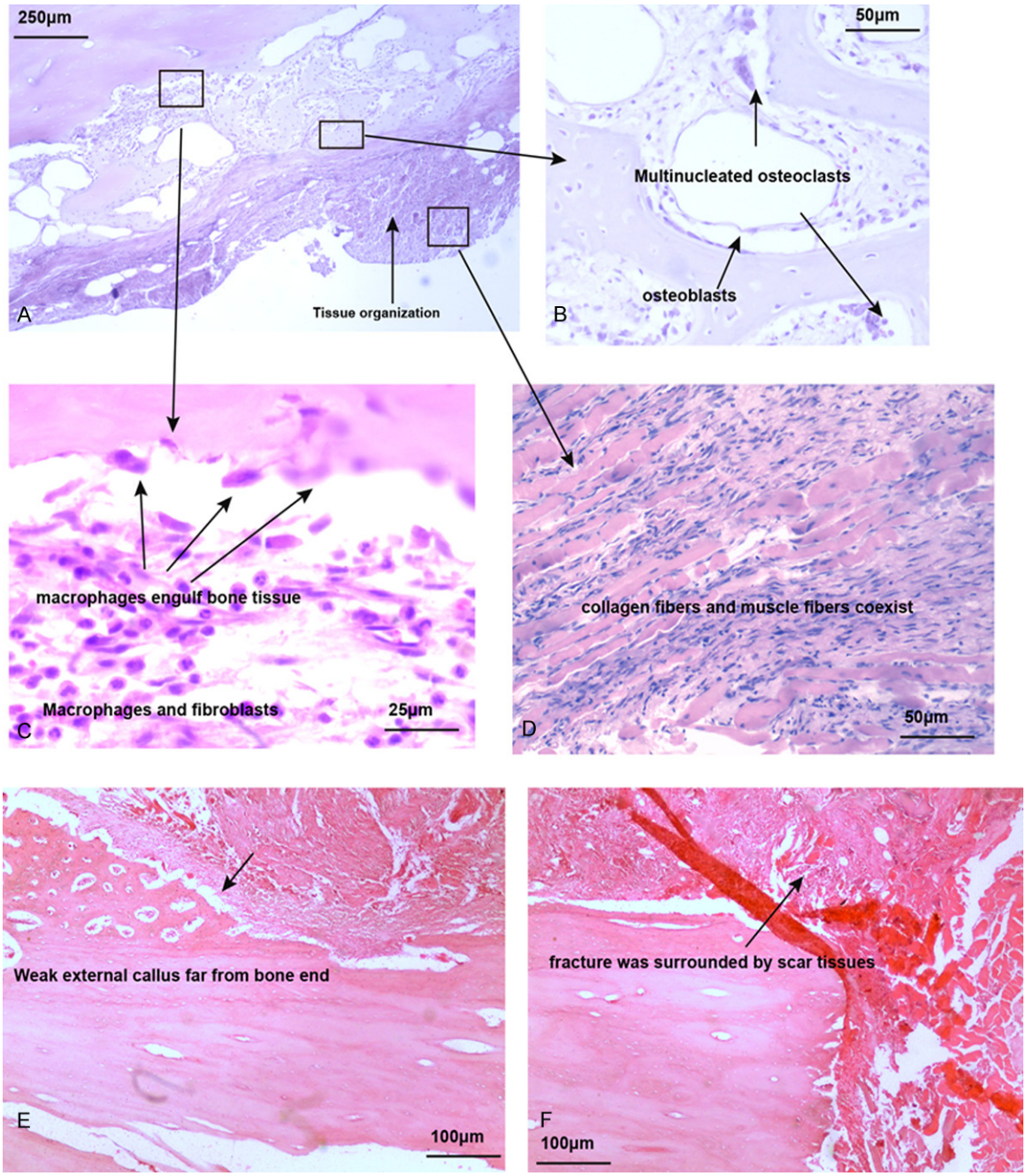

Figure 2. Tissue sections 28 d after the fracture. A-D. 14 d after the second operation of the group. A. The interface between bone and tissue organization shows a thin layer of cartilage and trabecular bone along the bone surface. H&E staining (40×). B. Multinucleated osteoclasts in the new callus follow a large number of osteoblasts at the edge of the trabecular bone, similar to the coupling of bone formation to resorption. H&E staining (200×). C. Macrophages and fibroblasts. A large number of macrophages and fibroblasts in the trabecular space; macrophages near the edge of the bone are enlarged and extracted osteoinductive factors to induce adjacent fibroblasts into chondrocytes or osteoblasts. H&E staining (40×). D. Collagen fibers and muscle fibers coexisted. H&E staining (40×). E, F. There was no secondary injury in the early operation group. There was no osteophyte growth mechanism in the adjacent tissue and fracture space at 4 weeks after the operation. There was no coupling of bone formation to resorption behavior, but only a scar growth mechanism. E. A small amount of weak external callus (coupling of bone formation to resorption) is initiated outside the cortical bone far from the end of the bone, which can slowly remodel the bone end representing direct healing in the bone end. It can directly heal the unstressed bone piece and the fractured end, but it cannot grow to the scar gap and adjacent tissues. H&E staining (40×). F. Scar tissues surround the end of the bone and the fracture. H&E staining (40×).

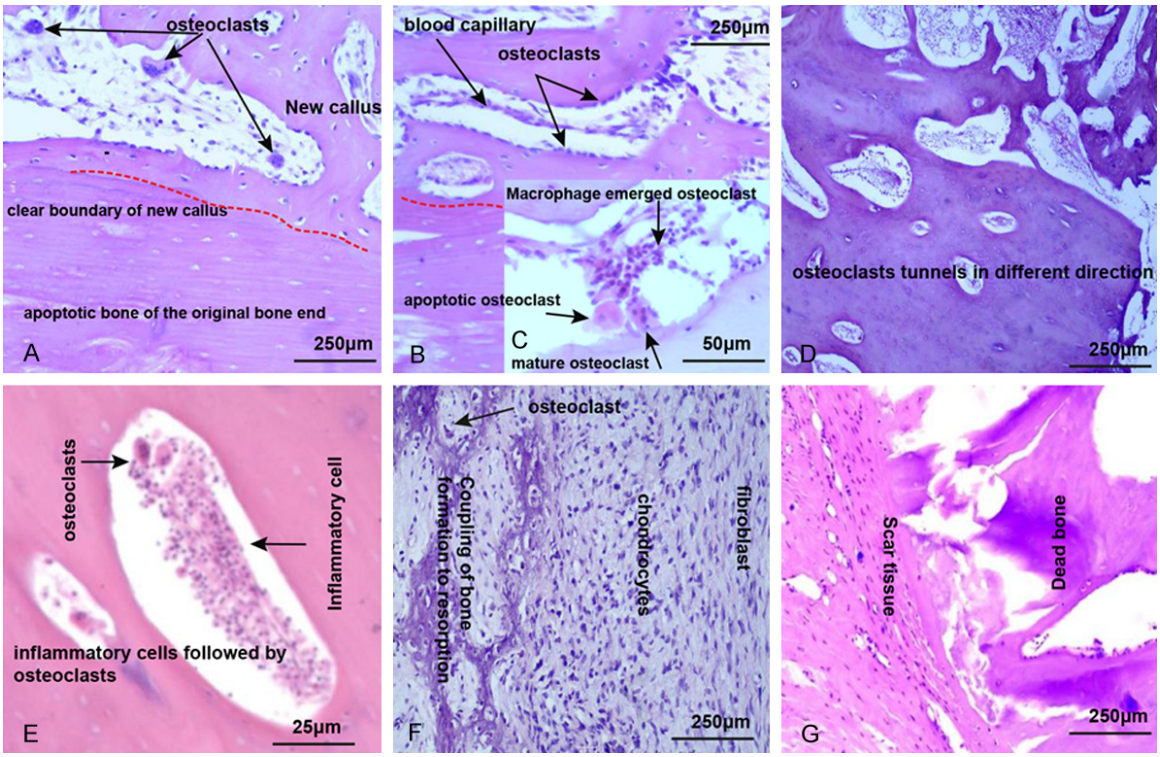

Figure 3. Tissue sections 42 d after the fracture. A-G. 28 days after the second operation in group A, no secondary injury was observed in group B. A, B. The new callus was located at the periphery of the bone end and closely combined with the apoptotic bone of the original bone end. The boundary between them is also very clear. Osteoclasts are on one side of the inner surface of the new trabecular bone, and the opposite side has many scattered osteoblasts, with inflammatory cells, fibroblasts, and capillaries in trabecular space. This is similar to Frost's coupling of bone formation to resorption, constituting a large new osteoblast-induced growth system. H&E staining (40×). C. Multiple mononuclear cell aggregations in the new trabecular space are new osteoclasts, as well as mature osteoclasts and senescent apoptotic osteoclasts. H&E staining (200×). D. Osteotylus reconstruction of apoptotic bone. Cutting cones of osteoclasts in different directions is destroying apoptotic bones, forming "tunnels" in a different direction, locking the callus with the three fractured ends. H&E staining (40×). E. Cutting cones of osteoclasts are enlarged, and the osteoclasts follow the inflammatory cells. H&E staining (400×). F. The process of fibroblasts causing bone-like osteophytes: fibroblasts-chondrocytes-bony trabecule (coupling of bone formation to resorption group), the result of the gradual transformation, is the growth of osteophytes into tissue organization. H&E staining (40×). G. The dead bone interface of scars in the early group. H&E staining (40×).

[14, 15]. Chondrocytes did not directly transform into osteoblasts but initiated coupling of bone formation to resorption (**Figure 3F**) [16, 17].

Light microscopy results of H&E staining showed that one side of the trabecular bone surface was scattered with osteoclasts. Also, the contralateral side was scattered with osteoblasts, interstitial inflammatory cells, fibroblasts, and capillaries (**Figure 3A**, **3B**), similar to the coupling of bone formation to resorption proposed by Frost *et al*. At first, coupling of bone formation to resorption destroyed only the callus itself, and the callus continued to self-strengthen and grew in the direction of the granulation tissue, which met the contralateral side, and then the two fractured apoptotic bones were remodeled tunnel-like. The capillaries and osteoblasts were directed where the osteoclasts tunnels point to (**Figure 3D**), forming osteophytes in different directions, which locked osteophytes in on three sides and stabilized the fractured end.

Discussion

The secondary injury phenomenon was first reported in the 1950s when Borden and Smith [18] observed 24 cases of recurrent femoral

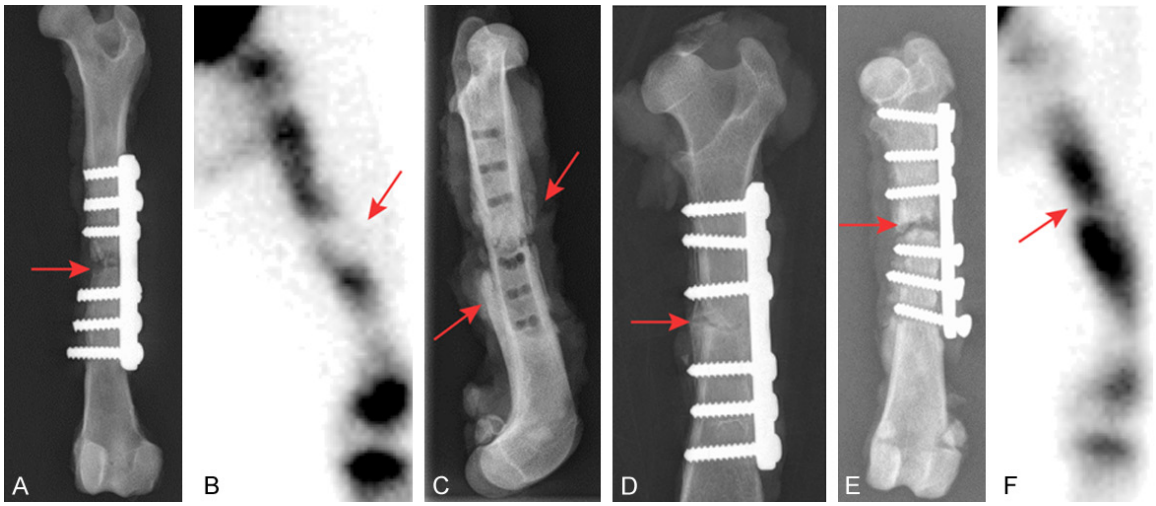

Figure 4. X-ray examination and radioisotope scanning of the affected limbs after the fracture to observe the growth of the callus and bone metabolism. A. Secondary injury group (group A), 14 days after the first surgery. X-ray examination showed no osteophyte growth in both groups (the results were comparable). B. Seven days after fracture, the radiologic scan showed a cold zone of bone metabolism of bone ends in both groups (the results were comparable). C. The bones were rapidly growing on both sides of the fracture 14 days after the second operation. D. The callus was healed 4 weeks after the second operation. E. In the early operation group (group B), there was no osteophyte growth, bone end absorption, or atrophic nonunion formation at 6 weeks after the operation, loose steel plates, or screw fractures. F. In the early operation group (group B), the cold zone of the radiologic scan was greatly reduced after 3 weeks.

fractures. They found that the callus growth after the second fracture was twice as fast as that of the first fracture, with average times of 37 days and 74 days, respectively. A decade later, Charnley *et al.* [19] reported 38 femoral fractures in 37 cases and found that the incidence of nonunion was 25% when surgery was carried out within 6 days after injury, and the incidence of nonunion was 7% when surgery was carried out 7 days after fracture. They suggested that postponing surgery could stimulate the process of bone regeneration for the second time. In 2015, Pan *et al.* [11] performed an experimental study to investigate the role of delayed operation in stimulating the growth of strong external callus in high-energy fractures and explored a new mechanism for bone healing. They found that the secondary injury can stimulate the growth of the callus. However, the above study only described the phenomenon of secondary injury but did not explore its cytological mechanism.

In this study, we performed a secondary injury of soft tissue exfoliation two weeks after the high energy fracture nonunion model was established (acute inflammation subsided). At that time, periosteum has lost the capacity for callus growth due to excessive inflammation damage. A secondary injury induced callus regrowth, suggesting that the secondary injury can restore fracture healing ability. The cytological data suggested that mild inflammation in the secondary injury combined with cascade reaction was initiated by macrophages, and mesenchymal stem cells initiated bone callus growth. This further suggested that surgical injury, i.e., mild inflammation, may also be beneficial to promote fracture healing at appropriate injury time.

It is well-known that fracture healing is initiated when an injury occurs. However, the direct response of tissue to injury is inflammation, so the fracture healing process must start with the inflammatory process [6-9, 27]. In this study, "benign" inflammation was induced through local re-injury of adjacent fracture tissues, which then initiated callus re-growth. Inflammation stimulated macrophages in adjacent tissues (**Figure 1A**, a simultaneous proliferation of mesenchymal stem cells 29), which engulfed bone tissue, caused transcription of bone-inducing factors in the BMP-2 signaling pathway (**Figures 2A-D**, **3**), and in turn, initiated callus growth. A certain proportion of macro-

phages adaptively transform into osteoclasts (**Figure 3A-F**) with hard bone tissue or cartilage tissue, after which osteoclast coupling factor [8, 14-17] was generated [16, 17] (**Figure 3A-F**), stimulating new bone callus formation. After growth of callus was initiated around the bone end and the fracture gap, stagnant bone restarted to grow. A previous study showed that macrophages at a fractured end are a source of BMP [14, 15] and can release TGF-β1 by osteoblastic cell efferocytosis [20] (**Figure 2C**). It is obvious that secondary injury does not increase blood supply or increase stability; yet, it induces mild re-inflammation and the recruitment of inflammatory macrophages and mesenchymal stem cells in the micro-environment. In recent years, a large number of studies have found that removing macrophages in the local fracture can cause fracture healing disorders [28-30]. Our results showed that excessive inflammation (in group B) could not recruit macrophages in adjacent tissues but could affect bone healing. Secondary injury (in group A) inflammation re-recruits inflammatory macrophages based on the destruction of adjacent tissues, restarting fracture healing, thus indicating that surgery should be postponed [10]. Moreover, a secondary injury may provide an operable and effective clinical approach to promote fracture healing. In this way, the inflammatory macrophages in the adjacent tissues engulf the bone-end bone cells, which effectively transcribe the bone-inducing signal substance to initiate the first callus and lead to bone-end cell apoptosis [10]. This process is regulated by four major cascade reactions, i.e., recruitment of inflammatory macrophages--mesenchymal stem cells and collagen hyperplasia--initiation of callus growth--apoptosis of old bone cells under the callus. Previous studies have shown that macrophages could regulate the differentiation of monocytes into osteoclasts or bone marrow mesenchymal stem cells (MSCs) into osteoblasts by TNF-α, IL-1β, and IFN-γ [7, 21-23]. Macrophages can also regulate the proliferation and migration of bone marrow mesenchymal stem cells, which is consistent with the results of this study.

Previous studies [10], together with our results, suggest that the primary injury inflammatory process overlaps with the surgical injury inflammatory process after early surgery of a high-energy fracture. Excessive inflammation produced in the early stage can inhibit the recruitment of macrophage cells and mesenchymal stem cells, impairing healing ability. Delayed surgery separates the primary inflammatory process from the surgical inflammatory process, breaking down one excess inflammation into two mild inflammations, two macrophages recruitment, and two initiating fracture healing processes, transforming surgical approach injury that impairs healing into a re-initiated secondary wound healing response. It is generally believed that injury of the periosteum and muscles tends to impair the ability to heal fractures; however, in this study, we restarted the fracture healing by timely using a secondary injury.

In the secondary injury group, the excessive inflammation subsided within 14 days. However, the healing response ability for inflammation was just recovered, and during that time the blocking scar tissue was not yet formed. The mild inflammation recruited macrophages and mesenchymal stem cells and restarted fracture healing. This further suggested that excessive inflammation of the local tissue of the fracture may lead to atrophic nonunion, which can be the best complement to the theory of "single blood supply failure leading to atrophic nonunion". This also proves that the actual effect of minimally invasive surgery is not to simply protect the blood supply. More importantly, it reduced the inflammatory response, thus providing new insight into the protection of inflammation in high-energy fractures to prevent nonunion. Bastian *et al.* and Bleak *et al.* suggested that inflammatory cells activate the fracture healing cascade [8, 9]. Yet, our data suggested that only mild inflammation can effectively activate macrophages to initiate fracture healing, which, on the other hand, was not observed for severe/excessive inflammation.

Richard *et al.* created a common low-energy fracture model and found that bone growth was accelerated in the early stages after surgery, but no difference was found in long-term effects [24]. In the current study, we focused on high-energy fractures with severe soft tissue injury-excessive inflammation in the early stage of the injury impaired fracture healing, while secondary injury restarted callus growth. A phenomenon of boneless growth without treatment errors as a biologic healing failure sug-

gested by Frost [25] postulates that secondary injury appears during the first operation. Yet, studying this phenomenon *in vivo* is challenging because experimental animals used for researches rarely suffer from biologic healing failure [25]. This study reproduced the secondary injury phenomenon by stabbing adjacent muscles to elicit this "no treatment error" animal model.

In the current study, we found the growth pattern of new osteophytes is destructive growth, for both necrotic bone end transformation and growth of new bone defects. While the osteoclasts destroy the cartilage or dead bone, cell osteogenesis induces new bone formation characterized by the coupling of bone formation to resorption. The essence of initiating the growth of the callus is to initiate the coupling of bone formation for resorption near the end of the bone. Chondrocytes and osteoblasts are first formed at the interface between bone and tissue organization since only bone tissue can provide osteoinductive substances (**Figure 3A**, **3B**). Bone-like osteophytes are produced outside the cortical bone, which is tightly bound to bone tissue. Meanwhile, there is no new bone formation in the original bone end, with no blood vessel growth, and the original bone cell apoptosis (**Figure 3A**, **3B**). The changes on surface of the callus are a gradual process of fibroblasts to chondrocytes to bone trabeculae (**Figure 3F**), indicating that fiber osteogenesis also undergoes a rapid cartilage stage. Inside the callus, a rich osteoclast population appears, followed by osteoblasts, which cause a coupling of bone formation to a resorption group [8, 17] (**Figure 3A**, **3B**), thus indicating that the chondrocytes do not directly transform into osteoblasts. This result suggested that the initial process of the new callus involves fibroblasts that are induced to produce cartilage and then immediately enter the coupling of bone formation to resorption. The coupling of bone formation to a resorption model is the most basic mode of fracture growth, which is more active in the new bone callus. The inner surface of the new trabecular bone is scattered with osteoclasts and a large number of osteoblasts, with a large number of macrophages and mesenchymal stem cells in the trabecular space, as well as fibroblasts and capillaries (**Figure 3A**, **3B**; **Table 4**), forming the true osteogenic induction interface. Many new bony trabeculae enlarge the bone growth area and constitute a huge bone growth system.

The failure of fracture healing is the failure of inflammation chemotaxis of mononuclear-macrophage-osteoclasts, which leads to failure of coupling of bone formation to resorption. Mononuclear-macrophage re-supply can re-initiate the callus growth (coupling of bone formation to resorption). Secondary injury inflammation can initiate this process because it can provide precursor cells (monocytes) and the most suitable environment for osteoclast genesis. The degradation products of osteoclasts in the new bone callus dissolve the trabecular bone matrix to stimulate the body to produce a "mild inflammatory absorption and repair reaction", so that the microvasculature is regenerated mononuclear-macrophages, and stem cells in the trabecular bone space can be continuously supplied (**Figure 3A-E**). Stem cells are continuously induced into osteoblasts, while macrophages engulf degradation products and continue to fuse into new osteoclasts, constantly replacing aging osteoclasts. Coupling of bone formation to resorption is constantly produced, forming the motive force for continuous growth and reconstruction of callus. This "microvascular inflammatory macrophage supply repair mechanism" constitutes the biologic basis of coupling of bone formation to resorption. Coupling of bone formation to resorption induces cartilage to become ossified, so the callus grows, strengthens itself, and grows in the direction of the granulation tissue, which meets the contralateral side, and then the two fractured apoptotic bones are remodeled tunnel-like. The capillaries and osteoblasts are directed where the osteoclasts tunnels point to (**Figure 3D**), forming osteophytes in different directions, which lock osteophytes with the two-fracture end in three sides and stabilize the fracture end.

Conclusion

This study suggests that for high-energy fractures and other nonunion high-risk cases, minimally invasive surgery or elimination of fracture space by open bone graft should be performed as early as possible before the mechanical stability is lost and aseptic inflammation is initiated. This secondary inflammation can re-initiate the growth of callus, and increase the bone healing effect compared to a bone graft itself,

thus preventing it from developing into atrophic nonunion from an early stage. This study promotes the development of a more accurate atrophic bone non-union model.

Acknowledgements

This study was funded by the 2016 Shaanxi Science and Technology Research Project (2016SF-291). We thank the electron microscope room and the animal laboratory of Xi'an Jiaotong University for their full cooperation.

Disclosure of conflict of interest

None.

Address correspondence to: Zhijun Pan, The 4th Hospital of Yulin City, 33 West Renmin Road, Yuyang District, Yulin City 719000, Shaanxi, China. Tel: +86-15191247732; E-mail: ylpanzhijun@163.com; Zhi Yuan, The Air Force Military Medical University, Xi'an 710032, Shaanxi, China. Tel: +86-13363976929; E-mail: xijingyiyuanyz@163.com

References

[1] Copuroglu C, Calori GM and Giannoudis PV. Fracture non-union: who is at risk? Injury 2013; 44: 1379-1382.

[2] Rupp M, Biehl C, Budak M, Thormann U, Heiss C and Alt V. Diaphyseal long bone nonunions - types, aetiology, economics, and treatment recommendations. Int Orthop 2018; 42: 247-258.

[3] Yu L and Fenglin Z. High-energy tibial plateau fractures: external fixation versus plate fixation. Eur J Orthop Surg Traumatol 2015; 25: 411-423.

[4] Westgeest J, Weber D, Dulai SK, Bergman JW, Buckley R and Beaupre LA. Factors associated with development of nonunion or delayed healing after an open long bone fracture: a prospective cohort study of 736 subjects. J Orthop Trauma 2016; 30: 149-155.

[5] Reed AA, Joyner CJ and Brownlow HC. Human atrophic fracture nonunions are not avascular. J Orthop Res 2002; 20: 593-599.

[6] Bastian O, Pillay J, Alblas J, Leenen L, Koenderman L and Blokhuis T. Systemic inflammation and fracture healing. J Leukoc Biol 2011; 89: 669-673.

[7] Loi F, Cordova LA, Pajarinen J, Lin TH, Yao Z and Goodman SB. Inflammation, fracture and bone repair. Bone 2016; 86: 119-130.

[8] Schmidt-Bleek K, Schell H, Lienau J, Schulz N, Hoff P, Pfaff M, Schmidt G, Martin C, Perka C, Buttgereit F, Volk HD and Duda G. Initial immune reaction and angiogenesis in bone healing. J Tissue Eng Regen Med 2014; 8: 120-130.

[9] Schmidt-Bleek K, Schell H, Schulz N, Hoff P, Perka C, Buttgereit F, Volk HD, Lienau J and Duda GN. Inflammatory phase of bone healing initiates the regenerative healing cascade. Cell Tissue Res 2012; 347: 567-573.

[10] Pan Z, Pan J, Wang H, Yu Z, Li Z, Yang W, Li J, Zhu Q and Luo Z. Healing physiology following delayed surgery for femoral midshaft fracture caused by high-energy injury: an in vivo study in dogs. J Int Med Res 2019; 47: 5155-5173.

[11] Pan ZJ, Li Z and Li J. Experimental study of high-energy fractures delayed operation in promote bone healing. Int J Clin Exp Med 2015; 8: 10619-10625.

[12] Julier Z, Park AJ, Briquez PS and Martino MM. Promoting tissue regeneration by modulating the immune system. Acta Biomater 2017; 53: 13-28.

[13] Brinkmann V, Reichard U, Goosmann C, Fauler B, Uhlemann Y, Weiss DS, Weinrauch Y and Zychlinsky A. Neutrophil extracellular traps kill bacteria. Science 2004; 303: 1532-1535.

[14] Garimella R, Tague SE, Zhang J, Belibi F, Nahar N, Sun BH, Insogna K, Wang J and Anderson HC. Expression and synthesis of bone morphogenetic proteins by osteoclasts: a possible path to anabolic bone remodeling. J Histochem Cytochem 2008; 56: 569-577.

[15] El-Jawhari JJ, Jones E and Giannoudis PV. The roles of immune cells in bone healing; what we know, do not know and future perspectives. Injury 2016; 47: 2399-2406.

[16] Sims NA and Martin TJ. Coupling signals between the osteoclast and osteoblast: how are messages transmitted between these temporary visitors to the bone surface? Front Endocrinol (Lausanne) 2015; 6: 41.

[17] Pettit AR, Chang MK, Hume DA and Raggatt LJ. Osteal macrophages: a new twist on coupling during bone dynamics. Bone 2008; 43: 976-982.

[18] Borden JN and Smith WS. Refracture of the shaft of the femur. South Med J 1952; 45: 874-876.

[19] Charnley J. Delayed operation in the open reduction of fractures of long bones. The Journal of Bone and Joint Surgery 1961; 43: 664-671.

[20] Michalski MN, Koh AJ, Weidner S, Roca H and McCauley LK. Modulation of osteoblastic cell efferocytosis by bone marrow macrophages. J Cell Biochem 2016; 117: 2697-2706.

[21] Chan JK, Glass GE, Ersek A, Freidin A, Williams GA, Gowers K, Espirito Santo AI, Jeffery R, Otto WR, Poulsom R, Feldmann M, Rankin SM, Horwood NJ and Nanchahal J. Low-dose TNF aug-

ments fracture healing in normal and osteoporotic bone by up-regulating the innate immune response. EMBO Mol Med 2015; 7: 547-561.
[22] Alexander KA, Chang MK, Maylin ER, Kohler T, Muller R, Wu AC, Van Rooijen N, Sweet MJ, Hume DA, Raggatt LJ and Pettit AR. Osteal macrophages promote in vivo intramembranous bone healing in a mouse tibial injury model. J Bone Miner Res 2011; 26: 1517-1532.
[23] Park JE and Barbul A. Understanding the role of immune regulation in wound healing. Am J Surg 2004; 187: 11s-16s.
[24] Coutts RD, Woo SL, Boyer J, Doty D, Gonsalves M, Amiel D and Akeson WH. The effect of delayed internal fixation on healing of the osteotomized dog radius. Clin Orthop Relat Res 1982; 254-260.
[25] Frost HM. The biology of fracture healing, part i and part II. Clin Orthop Relat Res 1989; 248: 283-309.
[26] Pajarinen J, Lin T, Gibon E, Kohno Y, Maruyama M, Nathan K, Lu L, Yao Z and Goodman SB. Mesenchymal stem cell-macrophage crosstalk and bone healing. Biomaterials 2019; 196: 80-89.
[27] Bahney CS, Zondervan RL, Allison P, Theologis A, Ashley JW, Ahn J, Miclau T, Marcucio RS and Hankenson KD. Cellular biology of fracture healing. J Orthop Res 2019; 37: 35-50.
[28] Schlundt C, El Khassawna T, Serra A, Dienelt A, Wendler S, Schell H, van Rooijen N, Radbruch A, Lucius R, Hartmann S, Duda GN and Schmidt-Bleek K. Macrophages in bone fracture healing: their essential role in endochondral ossification. Bone 2018; 106: 78-89.
[29] Baht GS, Vi L and Alman BA. The role of the immune cells in fracture healing. Curr Osteoporos Rep 2018; 16: 138-145.
[30] Batoon L, Millard SM, Raggatt LJ and Pettit AR. Osteomacs and bone regeneration. Curr Osteoporos Rep 2017; 15: 385-395.